

Electronic Supplementary Material

Modelling Permeation Passive Sampling: Intra-Particle Resistance to Mass Transfer and Comprehensive Sensitivity Analysis

Faten Salim,^a Marios Ioannidis^b, Alexander Penlidis,^b and Tadeusz Górecki^{*a}

^a University of Waterloo, Department of Chemistry, 200 University Avenue West, Waterloo, ON, Canada N2L 3G1.

^b University of Waterloo, Department of Chemical Engineering, 200 University Avenue West, Waterloo, ON, Canada N2L 3G1.

* Corresponding author. Email: tgorecki@uwaterloo.ca, Tel: +1 519 888 4567.

Numerical method to solve PDEs of mass transfer inside the particle

The radial distance along the particle radius is discretized into $z + 1$ points with the thickness of the resultant finite sections equal to $\Delta r = R/z$, as shown in Figure S1: Cross section of the discretized particle; therefore, the distance r_k at each point k from the center of the sphere, where $k = 1, 2, \dots, z+1$, can be expressed as follows:

$$r_k = [(z + 1) - k]\Delta r \quad (S1)$$

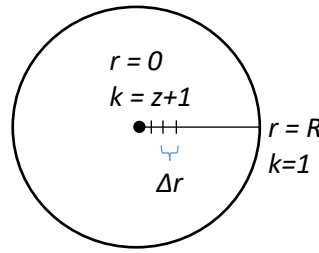


Figure S1: Cross section of the discretized particle

At each point k one can write:

$$\begin{aligned} \frac{1}{r_k^2} \frac{\partial}{\partial r} \left(r^2 \frac{\partial C_p}{\partial r} \right) \Big|_{r=r_k} &= \frac{\partial^2 C_p}{\partial r^2} \Big|_{r=r_k} + \frac{2}{r_k} \frac{\partial C_p}{\partial r} \Big|_{r=r_k} \\ &\approx \frac{C_{p(k+1)} - 2C_{p(k)} + C_{p(k-1)}}{(\Delta r)^2} + \left(\frac{2}{[(z+1) - k]\Delta r} \right) \left(\frac{C_{p(k+1)} - C_{p(k-1)}}{2\Delta r} \right) \end{aligned} \quad (S2)$$

The above means that Equation 5 for points $1 < k < z+1$ becomes:

$$\begin{aligned} \varepsilon_\mu \frac{dC_{p(k)}}{dt} &= D_p \left[\frac{C_{p(k+1)} - 2C_{p(k)} + C_{p(k-1)}}{(\Delta r)^2} + \left(\frac{2}{[(z+1) - k]\Delta r} \right) \left(\frac{C_{p(k+1)} - C_{p(k-1)}}{2\Delta r} \right) \right] - (1 \\ &\quad - \varepsilon_\mu) \left(\frac{dq_{p(k)}}{dt} \right) \end{aligned} \quad (S3)$$

Based on Eq. 7, one can write:

$$\frac{dq_{p(k)}}{dt} = k(1/n)C_p^{\left(\frac{1}{n}-1\right)} \frac{dC_{p(k)}}{dt} \quad (S4)$$

Therefore, Eq. S3 can be re-written as follows:

$$\begin{aligned} \varepsilon_\mu \frac{dC_{p(k)}}{dt} + (1 - \varepsilon_\mu)k(1/n)C_p^{\frac{1}{n}-1} \frac{dC_{p(k)}}{dt} \\ = D_p \left[\frac{C_{p(k+1)} - 2C_{p(k)} + C_{p(k-1)}}{(\Delta r)^2} + \left(\frac{2}{[(z+1) - k]\Delta r} \right) \left(\frac{C_{p(k+1)} - C_{p(k-1)}}{2\Delta r} \right) \right] \end{aligned} \quad (S5)$$

The first term in the left-hand side of Eq. S5 is negligible compared to the second term (k is a large number); thus, this equation can be restated as follows:

$$\frac{dC_{p(k)}}{dt} = \left(\frac{D_p C_p^{(1-\frac{1}{n})}}{(1 - \varepsilon_\mu)k(\frac{1}{n})} \right) \left[\frac{C_{p(k+1)} - 2C_{p(k)} + C_{p(k-1)}}{(\Delta r)^2} + \left(\frac{2}{[(z+1) - k]\Delta r} \right) \left(\frac{C_{p(k+1)} - C_{p(k-1)}}{2\Delta r} \right) \right] \quad (S6)$$

At the center of the particle, using Taylor approximation about $r = 0$, one can write:

$$\frac{1}{r} \frac{\partial C_p}{\partial r} \approx \frac{\partial^2 C_p}{\partial r^2} \Rightarrow \frac{\partial^2 C_p}{\partial r^2} + \frac{2}{r} \frac{\partial C_p}{\partial r} = 3 \frac{\partial^2 C_p}{\partial r^2} \quad (S7)$$

Also, from the boundary condition in Eq. 9,

$$\left. \frac{\partial C_p}{\partial r} \right|_{r=0} \approx \frac{C_{p(z+2)} - C_{p(z)}}{2\Delta r} = 0 \Rightarrow C_{p(z+2)} \approx C_{p(z)} \quad (S8)$$

From Eq. 5 and Eq. S7, it can be concluded that at the center of the particle where $r = 0$ and $k = z+1$, the differential equation becomes:

$$\varepsilon_\mu \frac{dC_{p(z+1)}}{dt} = 3D_p \left[\frac{C_{p(z+2)} - 2C_{p(z+1)} + C_{p(z)}}{(\Delta r)^2} \right] - (1 - \varepsilon_\mu) \left(\frac{dq_{p(z+1)}}{dt} \right) \quad (S9)$$

From Equations S9, S8, and S4, the equation at the center of the particle becomes:

$$\varepsilon_\mu \frac{dC_{p(z+1)}}{dt} + (1 - \varepsilon_\mu)k \frac{1}{n} C_p^{\frac{1}{n}-1} \frac{dC_{p(z+1)}}{dt} = 6D_p \frac{C_{p(z)} - C_{p(z+1)}}{\Delta r^2} \quad (S10)$$

The first term on the left-hand side of this equation is negligible compared to the second term; therefore, this equation can be re-written as follows:

$$\frac{dC_{p(z+1)}}{dt} = \left(\frac{6D_p C_p^{1-\frac{1}{n}}}{(1 - \varepsilon_\mu)k \frac{1}{n}} \right) \left(\frac{C_{p(z)} - C_{p(z+1)}}{\Delta r^2} \right) \quad (S11)$$

The solutions for the resultant ordinary differential equations (ODEs) were found using a MATLAB code (R2015a, MathWorks, USA), using ODE15s solver.

Calculating the average concentration inside the particle

After calculating the concentration at each node of the discretized particle, the number of free moles, M_{free} , in the finite volume (ΔV) defined by two nodes (k and $k+1$) is calculated as follows:

$$M_{free,\Delta V} = \frac{C_{p(k)} + C_{p(k+1)}}{2} \cdot \Delta V = \frac{C_{p(k)} + C_{p(k+1)}}{2} \cdot 4\pi \left(\frac{r_k + r_{k+1}}{2} \right)^2 \cdot \Delta r \quad (S12)$$

The total number of moles in the particle, $M_{free,V}$, was then calculated by summing the number of moles in the discrete volumes of the particle. Average concentration inside the particle, $C_{p(ave)}$, was calculated by dividing the total number of moles, $M_{free,V}$, by the average particle volume.

The free concentration gradient inside the particle at its surface, $\left. \frac{dC_p}{dr} \right|_{r=R}$ was approximated as follows:

$$\left. \frac{dC_p}{dr} \right|_{r=R} \approx \frac{C_{p(2)} - C_{p(1)}}{\Delta r} \quad (S13)$$

Table S1: Details of vapor concentrations and their measurement

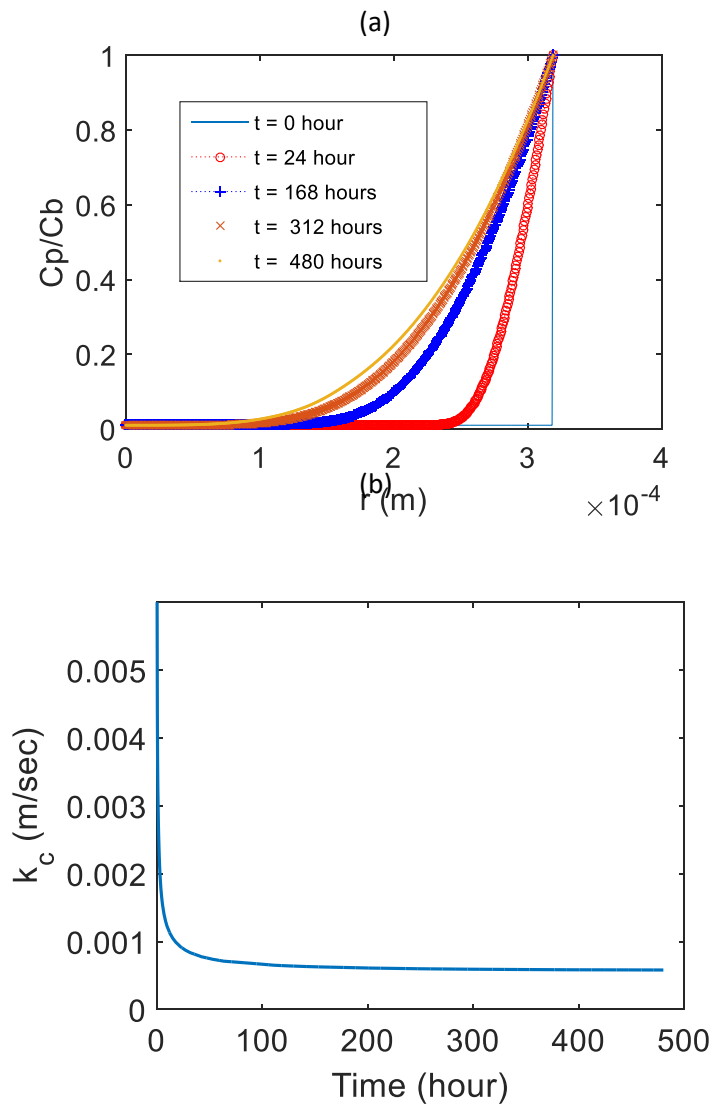
Experiment	Target analyte	Temperature of the vapor source (°C)	Adsorbent used in the sorption tube	Pumping tool	Volume sampled	Average measured concentration (mg/m ³)
1	TCE	40	Carbopack B	10-ml-gas-tight syringe	10 ml	8.96
			Anasorb 747	Sampling pump	1500 - 3040 ml	
2	Toluene	60	Anasorb 747	10-ml-gas-tight syringe	50 ml	6.81
3	TCE	60	Anasorb 747	10-ml-gas-tight syringe	50 ml	27.56

Table S2: Values of parameters used in the evaluation of the model results with Anasorb 747.[§]

Symbol	Description	Values corresponds to the sampled analyte	
		Toluene	TCE
L_m	Membrane thickness (m)	1.0×10^{-4}	2.0×10^{-4}
L_b	Sorbent bed thickness (m)		1.4×10^{-2}
A_m	Membrane sampling area (m ²)		34.5×10^{-6}
D_m	Diffusion coefficient in the membrane (m ² /sec)	1.35×10^{-10} (ref. ¹⁻⁶)*	1.3×10^{-10} (ref. 7)
K	Partition coefficient between air and the membrane material (dimensionless)	843 (ref. ^{8,9})*	900 (based on ref. ¹⁰)
D_a	Diffusion coefficient in air (m ² /sec)	8.50×10^{-6} (ref. ¹¹)	8.75×10^{-6} (ref. ¹²)
ϵ_μ	Particle porosity		0.45
D_b	Effective diffusion coefficient in the sorbent bed (m ² /sec)	1.44×10^{-6}	1.46×10^{-6}
ϵ or ϵ_M	Sorbent bed porosity (dimensionless)		0.40
τ	Tortuosity (dimensionless)		$\epsilon^{(-1/2)}$
α	Specific surface area (m ² /m ³)		629899050
k_c	Mass transfer coefficient (m/sec)	0.001	0.001
d	Sorbent particle diameter (m)		6.375×10^{-4}
a	Parameter for the isotherm $C^* = a \times q^b$	2.52×10^{-12}	4.77×10^{-16}
b	Parameter for the isotherm $C^* = a \times q^b$	2.44	3.59
r_p	Average pore radius (m)		5.84×10^{-10}
D_k	Knudsen diffusivity (m ² /sec)	1.01×10^{-7}	8.47×10^{-8}
$D_{p,eff}$	Effective pore diffusion coefficient (m ² /sec)	3.05×10^{-8}	2.56×10^{-8}
k	Parameter for the isotherm $q_p = kC_p^{\frac{1}{n}}$	57204	18335
$1/n$	Parameter for the isotherm $q_p = kC_p^{\frac{1}{n}}$	0.41	0.28

*An average value from the references listed

[§] Measurement and calculations of parameter values are presented in the sections "Measurement of the isotherm parameters" and "Characterization of Anasorb 747" of this supplementary information.



FigureS2: Propagation of the normalized free concentration profile of toluene inside the particle (a) and the calculated mass transfer coefficient, k_c , (b) with time.

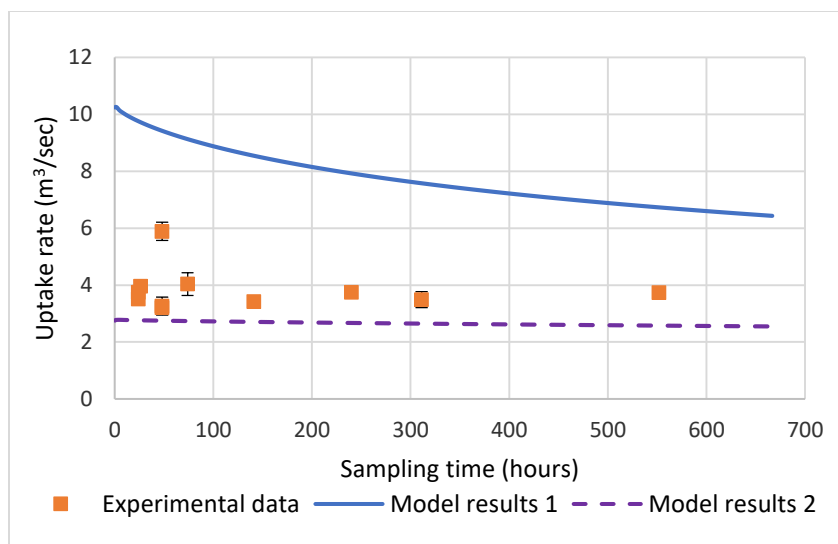


Figure S3: Comparison between the experimental uptake rate values for TCE with those obtained using the model when $K = 621$, while $D_m = 4.8 \times 10^{-10} \text{ m}^2/\text{s}$ (Model results 1) and $D_m = 1.3 \times 10^{-10} \text{ m}^2/\text{s}$ (Model results 2).

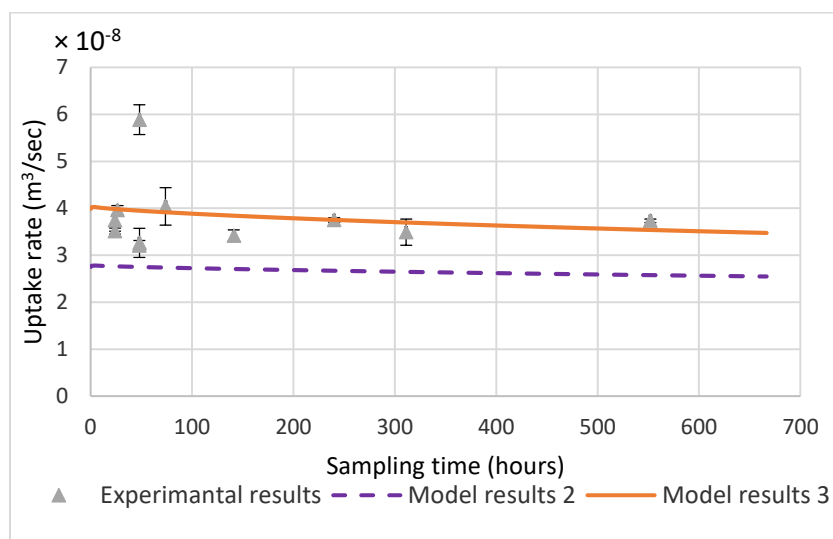


Figure S4: Comparison between the experimental uptake rate values for TCE with those obtained using the model when $D_m = 1.3 \times 10^{-10} \text{ m}^2/\text{s}$, while $K = 621$ (Model results 2) and $K = 900$ (Model results 3).

Initial sensitivity analysis (one-parameter-at-a-time)

This evaluation was conducted over a sampling time of up to 500 hours at a concentration of $0.00001 \text{ mol}/\text{m}^3$. The base set of parameters corresponded to “sampling” toluene vapor using WMS (with the PDMS membrane) containing Carboxpack B adsorbent. These values and the ranges used for selected parameters are presented in Table S3.

Table S3: Parameters involved in the initial sensitivity analysis and the ranges/values used for these parameters.

Symbol	Description	Sensitivity analysis	
		Base value	Range/Values
L_m	Membrane thickness (m)	1×10^{-4}	
L_b	Sorbent bed thickness (m)	1.4×10^{-2}	
A_m	Membrane sampling area (m ²)	34.5×10^{-6}	
D_m	Diffusion coefficient in the membrane (m ² /sec)	1.07×10^{-10} (ref. ¹⁻⁵)*	$1 \times 10^{-11} - 2 \times 10^{-10}$
K	Partition coefficient between air and the membrane material (dimensionless)	843 (ref. ^{8,9})*	150 - 10000
D_a	Diffusion coefficient in air (m ² /sec)	8.5×10^{-6} (ref. ¹¹)	$1.0 \times 10^{-6} - 1.0 \times 10^{-5}$
ϵ_μ	Particle porosity		
D_b	Effective diffusion coefficient in the sorbent bed (m ² /sec)	2.11×10^{-6}	$2.48 \times 10^{-7} - 1 \times 10^{-6}$
ϵ/ϵ_M	Sorbent bed porosity (dimensionless)	0.40	0.30, 0.40, 0.50
τ	Tortuosity (dimensionless)	1.61	
α	Specific surface area (m ² /m ³)	$11226 \times 10^{+4}$	
k_c	Mass transfer coefficient (m/sec)	0.0198	
d	Sorbent particle diameter (m)	2.135×10^{-4}	
a	Parameter for the isotherm $C^* = a \times q^b$	7.67×10^{-6} (ref. ¹³)	$7.67 \times 10^{-7}, 7.67 \times 10^{-6}, 7.67 \times 10^{-7}$
b	Parameter for the isotherm $C^* = a \times q^b$	1.566 (ref. ¹³)	1.466, 1.566, 1.866, 2.400

*An average value from the references listed

The results of this analysis are presented in Figure S5 and Figure S6. In Figure S5-A, changes in the uptake rate for a range of values of diffusivity in the membrane, D_m , are evaluated with sampling time. The results show high sensitivity to this parameter, which is mainly influential on the initial value of the uptake rate and the rate of its decrease with sampling time. Higher value of the diffusion coefficient in the membrane produces higher initial value of the uptake rate and higher rate of decrease over time. This can be explained by the fact that higher diffusivity in the membrane increases the flux of analyte molecules into the sorbent bed. If mass transfer parameters inside the sorbent bed do not change, increasing the flux into the bed increases the concentration in the gas phase at the interface between the membrane and the sorbent bed. Although this also increases the sorption rate, which initially increases the uptake rate, the free concentration at the bed interface with the membrane will increase more rapidly, leading to more rapid reduction in the uptake rate.

Figure S5-B presents the sensitivity of the uptake rate to the partition coefficient value between air and PDMS, K . The uptake rate is only sensitive to this parameter at the beginning of the sampling time. Shortly after, the uptake rate stabilizes, with no significant change as the partition coefficient value changes. This partition coefficient appears in the boundary conditions of the model; therefore, its effect is mainly on the concentration in the membrane at its interface with the outside air and on the free concentration in the sorbent bed at its interface with the membrane. The increase in the latter concentration as a result of the increase in K is expected to be the cause of the initial effect on the uptake rate. The influence of the diffusion coefficient in the sorbent bed, D_b , on the uptake rate over

time is demonstrated in Figure S5-C. It can be observed in this figure that increasing the diffusivity in the sorbent bed decreases the rate at which the uptake rate changes over the sampling time. This effect can be explained by the fact that higher diffusivity in the sorbent bed facilitates more efficient mass transfer within the bed, which reduces the concentration of the free analyte molecules at the interface of the sorbent bed with the membrane.

Figure S6 shows the results of the initial sensitivity analysis for the sorption isotherm parameters, a and b , and for the bed porosity, ε . From these three parameters, only the isotherm parameter, a , seems to be influential on the uptake rate value. It can be seen in Panel (A) of this figure that higher uptake rate values and smaller rate of decrease over time are obtained as a becomes smaller. This can be explained when evaluating the effect of the parameter, a , on the free concentration of the analyte, as presented in the isotherm in Table S2. Decreasing the isotherm parameter, a , increases the sorption rate and decreases the free concentration of the analyte in the sorbent bed, which maintains the concentration gradient between both sides of the membrane.

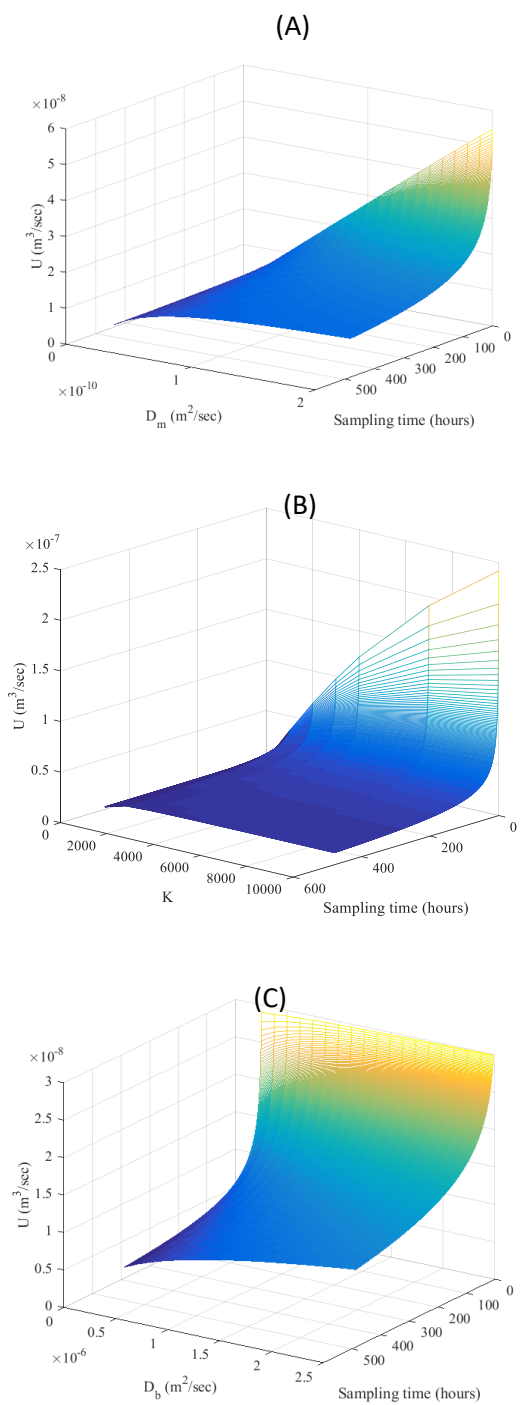


Figure S5: Results of the initial sensitivity analysis of the uptake rate towards the diffusivity in the membrane (A), the partition coefficient between air and PDMS (B), and the diffusivity in the sorbent bed (C).

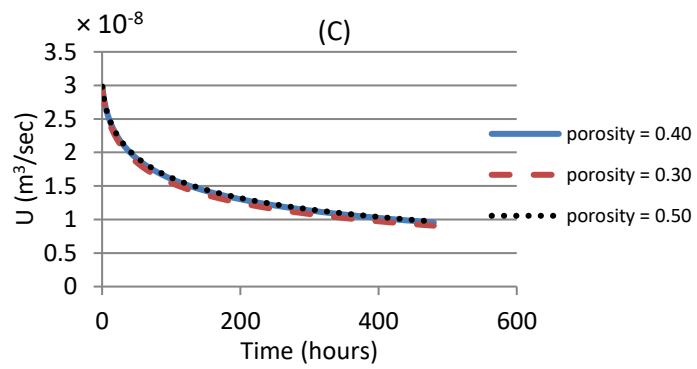
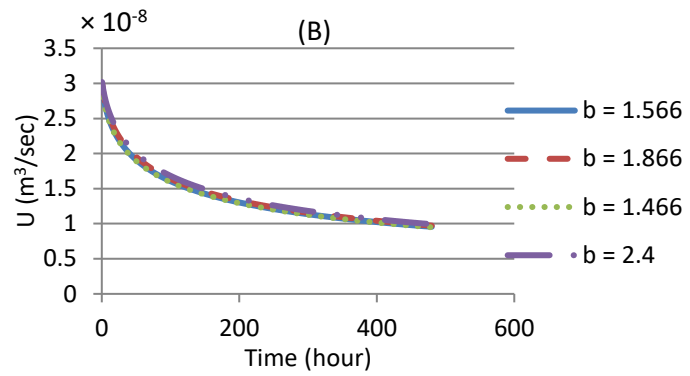
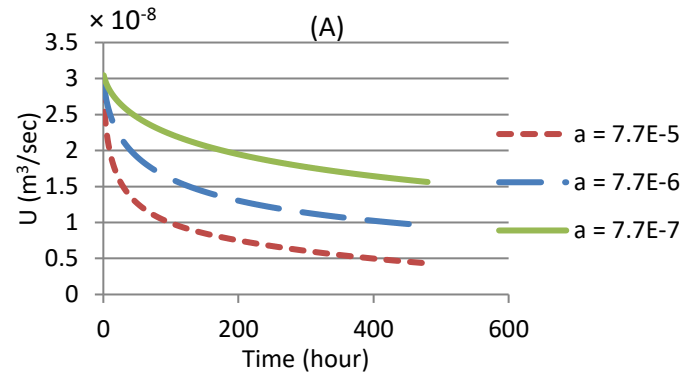


Figure S6: Results of the initial sensitivity analysis of the uptake rate towards the isotherm parameters a (A) and b (B), and the bed porosity (C).

Table S4: Values of input parameters used in the sensitivity analysis.

Parameter	Sorbent					
	Carbopack B			Anasorb 747		
	Base value	Lower bound	Upper bound	Base value	Lower bound	Upper bound
D_m (m ² /sec)	1×10^{-10}	1×10^{-11}	1×10^{-9}	1×10^{-10}	1×10^{-11}	1×10^{-9}
K	800	600	1000	800	600	1000
ϵ	10000	7500	12500	10000	7500	12500
k_c (m/sec)	0.40	0.36	0.44	0.40	0.36	0.44
b	0.02	-	-	0.001	0.0001	0.05
	1.566	1	2	3	2	4

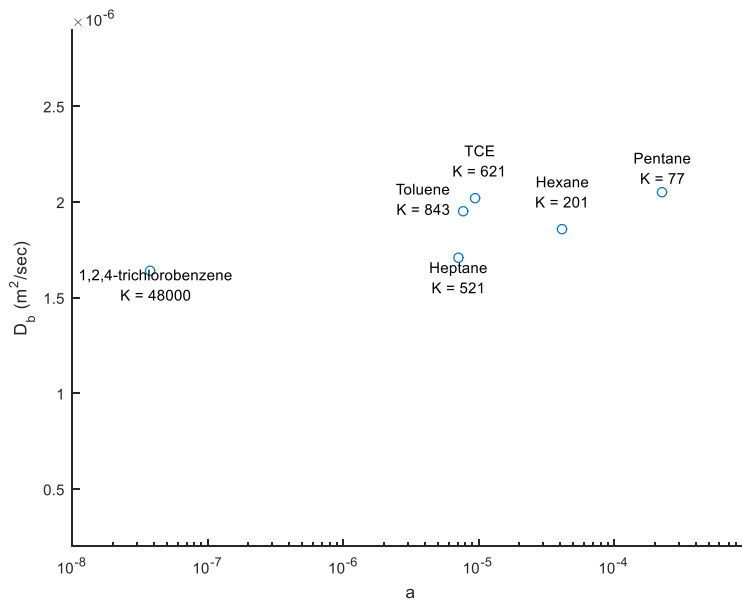


Figure S7: Distribution of a group of VOCs with different values of the partition coefficient, K , values within the parameter space of (D_b, a) .

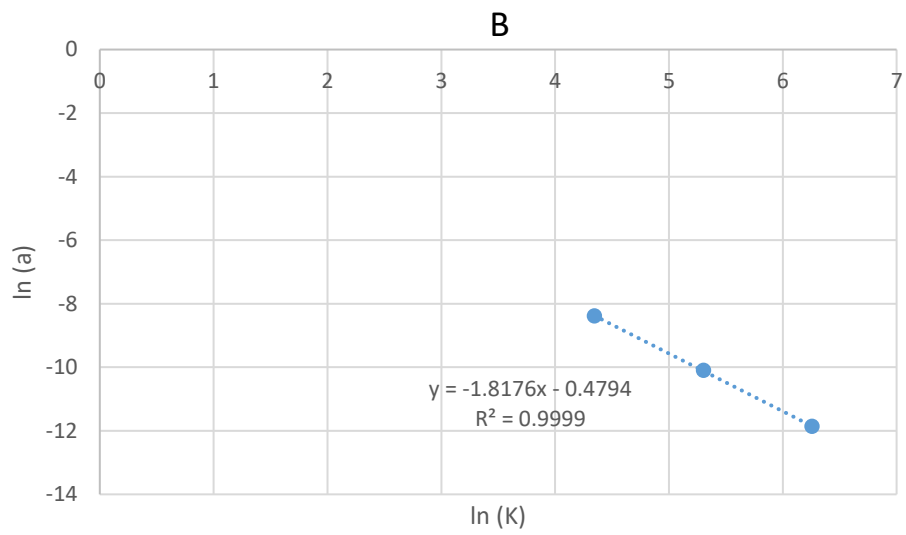
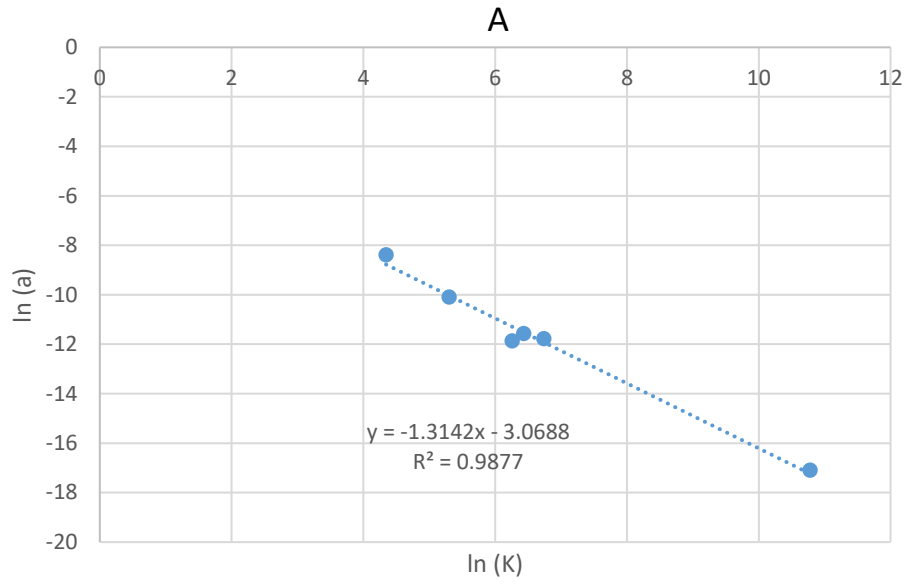


Figure S8: Observed correlations between the isotherm parameter, a , and the partition coefficient, K , for a group of VOCs (A) and for linear hydrocarbons (B).

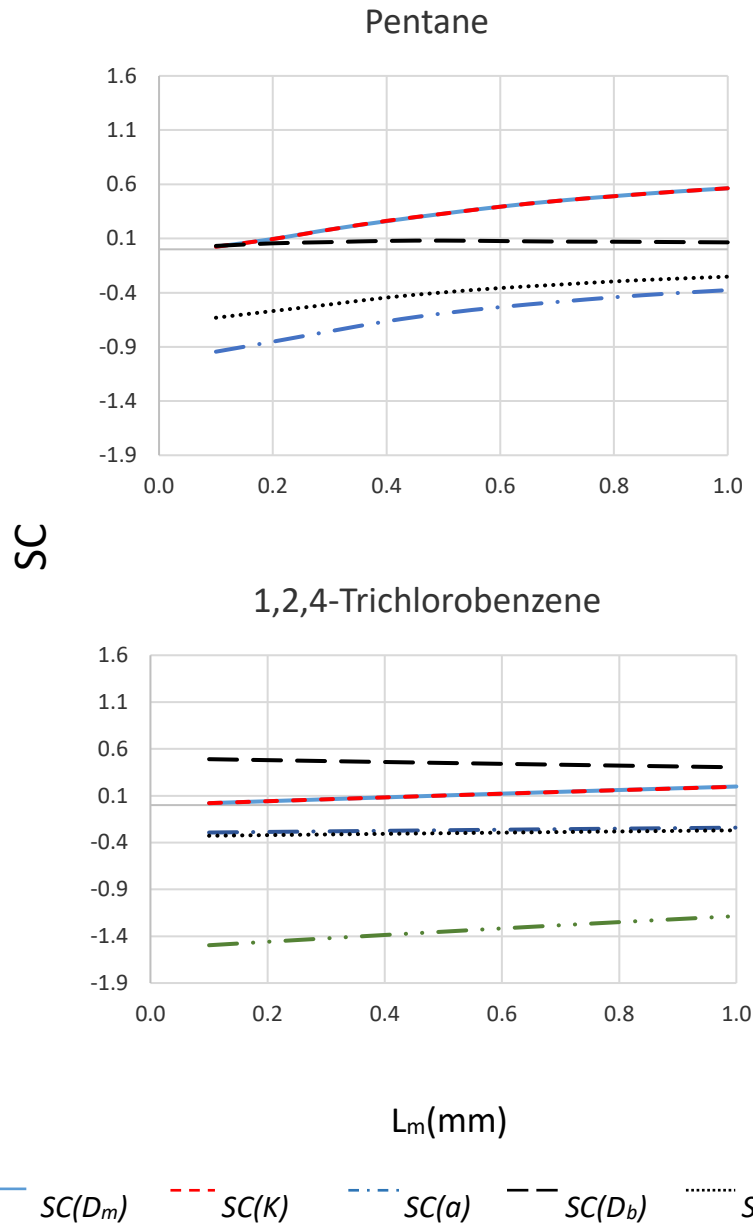


Figure S9: Sensitivity coefficients (SCs) as a function of the membrane thickness, L_m , for two analytes: pentane and 1,2,4-trichlorobenzene, when Carbopack B is used as a sorbent.

Determination of the isotherm parameters

Method

To determine the isotherm parameters, a and b , as presented in Table 1, the maximum capacities of the adsorbent at different gas concentrations were determined using the modified Wheeler equation:¹

$$t_b = \left(\frac{W_e}{C_o Q}\right) \left[W - \left(\frac{\rho_B Q}{k_v}\right) \ln\left(\frac{C_o - C_x}{C_x}\right) \right] \quad (S14)$$

In this equation, t_b is the breakthrough time (min), which is defined as the time needed for the standard gas to pass through the adsorbent bed before the analyte starts to elute from the bed, C_o is the inlet concentration (g/cm^3), W_e is the adsorption capacity (g/g), Q is the volumetric flow rate (cm^3/min), W is the weight of adsorbent (g), ρ_B is the bulk density of the bed (g/cm^3), k_v is the rate coefficient (min^{-1}), and C_x is the exit concentration (g/cm^3), which is a time-dependent concentration. The plot of t_b versus the adsorbent weight, W , at a given vapor concentration, C_o , when all other parameters are constant, produces a straight line with an equation of the form: $t_b = mW + B$. In this equation, m and B are the slope and intercept, respectively. The slope, m , can be expressed as follows:

$$m = \frac{W_e}{C_o Q} \quad (S15)$$

Eqn. S15 allows the calculation of the maximum capacity of the adsorbent, W_e , at a given concentration, C_o , if the flow rate, Q , is known.

In order to measure the breakthrough time at a given analyte concentration, the standard gas of that concentration was passed through a bed of the adsorbent with an accurately measured mass and at a controlled temperature. The flow rate of the standard gas through the bed was monitored during the experiment. The effluent was directed towards a detector to monitor the analyte at the outlet of the packed tube. The experiment continued until a breakthrough curve, similar to that presented in Figure S10, was obtained. The time at the intercept between the tangent of the curve at the inflection point with the abscissa was considered the breakthrough time.

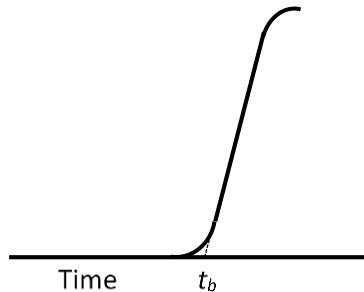


Figure S10: Breakthrough curve

The experiment was repeated at the same concentration level with different masses of the adsorbent in order to plot the changes in the breakthrough time with the adsorbent mass and obtain the slope described in eqn. S15. After determining the maximum adsorbent capacity at a given concentration, the procedure was repeated with different concentrations until enough points were collected to establish the isotherm equation.

Experimental setup

The setup illustrated in Figure S11 was used to measure the breakthrough time at a given concentration. In this setup, nitrogen gas, from a high-pressure source, was passed through an activated charcoal purifier. It was passed, afterwards, through a mass flow controller (MKS, Andover, MA, USA, 0-100 mL/min), the flow rate through which was set and monitored using an MKS 4-channel readout system (Andover, MA, Type 247). The nitrogen gas was passed through a vapor generator, which consisted of a flow-through vessel, containing an analyte vapor source, placed inside a GC oven to control the temperature. The analyte vapor source consisted of a diffusion source or a PTFE permeation source depending on the desired concentration level. The diffusion source consisted of a glass vial containing the analyte neat liquid. The vial was sealed with an open top cap and Teflon/Silicon septum or by a silicon stopper. A fused silica capillary (Restek guard column) was inserted through the cap septum or the stopper as a diffusion path. The length and the ID of the capillary varied within the ranges of 40 – 55 mm and 0.25 – 0.53 mm, respectively, depending on the volatility of the analyte and the desired concentration. For details about the PTFE permeation source, the reader is referred to Ref. ³. Changing the temperature of the vapor source was used as a method of adjusting the concentration. The oven temperature ranged between 40 °C and 90 °C. The standard gas was passed, afterwards, through an approximately 4 m long copper tube of a 1/8" OD to equilibrate the gas temperature with the ambient temperature before the gas was passed through the sorptive tube packed with a certain amount of the adsorbent. The tube used for this purpose was a stainless steel tube, 6.35 mm OD × 90 mm long, originally used in Perkin Elmer thermal desorption unit (ATD 400). The adsorbent, inside the tube, was packed in between two layers of glass wool (Fisher Scientific, Ottawa, ON, Canada) of approximately 1.5 cm thickness for each layer. The packed tube was kept at a constant temperature of 21 °C by placing it inside a thermostated chamber. This chamber consisted of a ten-liter, double-layer glass jar. The inner layer was wrapped with a copper tube connected to a circulating bath equipped with a programmable temperature controller (Model 1147P, VWR International, LLC, PA, USA). The chamber was also wrapped with an insulating layer and covered with a top plate consisting of two layers with

holes that allowed passing the tubes into and out of the chamber, and a thermometer to monitor the temperature inside. The inner layer of the top plate was a PTFE plate with an O-ring to provide good sealing with the edge of the glass jar, while the top layer consisted of a stainless steel plate. The flow through the packed tube was monitored using a rotameter (150 mm Flow Tube, Direct-Reading for 100 mL/min Nitrogen, Cole-Parmer Instrument Co., Montreal, Canada). The rotameter, seated on top of the chamber, was connected from one end to the packed tube, while the other end was connected to a ¼" PTFE tube. This tube was used to direct the effluent gas to a split point before entering the detector. A stainless steel tee connected to the PTFE tube was used for this purpose. One end of the Tee was connected to the FID detector using a 0.53-ID deactivated fused silica tube, while the other end was directed to the fume hood after passing through a needle valve to maintain enough pressure to force the flow into the detector. The flow through the packed tube was measured to be 103 ml/min, while the flow into the detector was 31 ml/min. The detector used in these experiments was an FID detector installed in a GC-FID instrument (FINNIGAN Focus GC, Thermo Scientific, USA).

A three-way stainless steel valve was connected before the packed tube to direct the flow through the tube (Line 1) or to the fume hood during concentration equilibration time (Line 2). The flow through Line 2 was passed through a needle valve to control the pressure, so that the pressure and, therefore, the flow rate were maintained when switching the flow between the two lines. Active sampling was conducted as a method for determining the standard gas concentration. Active samples were collected by switching the flow through Line 2 to pass through a sorption tube connected to a bubble flow meter on the opposite end, used to accurately determine the flow rate. Sorption tubes used for active sampling were packed with either Carboxpack B or Anasorb 747. Details about analysing both adsorbents can be found in the experimental section.

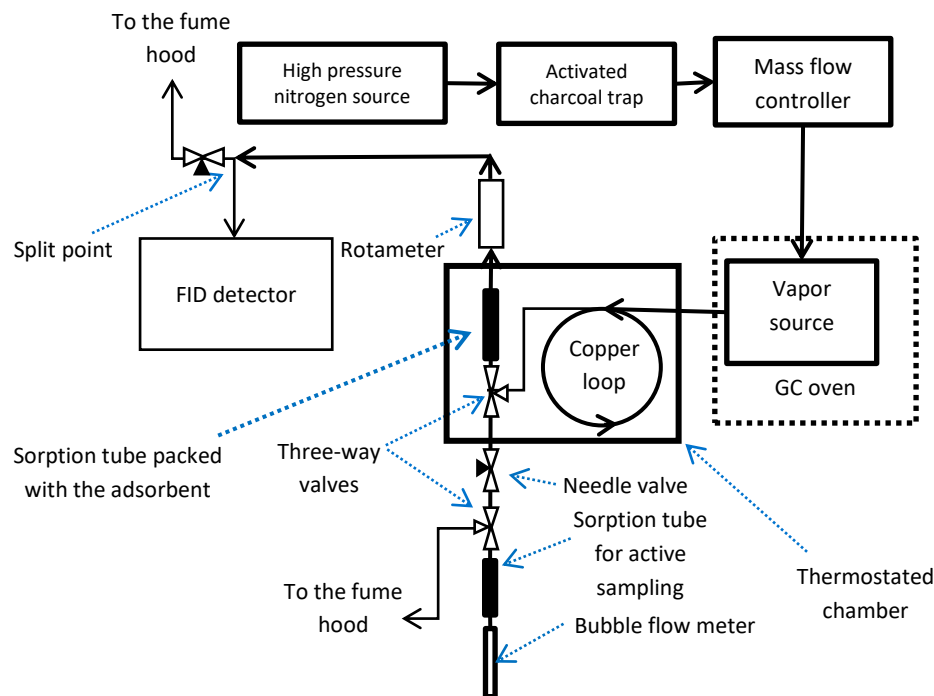


Figure S11: Experimental setup used in the breakthrough experiments

Results

The concentration of the sorbed analyte was determined by fitting the data points to the linearized Freundlich isotherm form presented in S16.

$$\log(q) = \log(K) + \frac{1}{n} \log(C) \quad (\text{S16})$$

In this equation, q and C are the concentrations of the sorbed analyte (mole per m^3 of the solid phase) and the concentration in the gas phase (mol/m^3), respectively. K and n are empirical constants.

The measurement included two types of adsorbents: Carbopack B and Anasorb 747. Carbopack B is a non-porous adsorbent with specific surface area of $100 \text{ m}^2/\text{g}$ (as provided by the manufacturer). The density of the solid particles was measured using a pycnometer: $\rho_s = 1.87 \pm 0.19 \text{ g}/\text{cm}^3$. Anasorb

747 is a highly porous adsorbent with a specific surface area 1145 m²/g (see details in the next section). The solid density was calculated to be $\rho_s = 1.47 \text{ g/cm}^3$ (calculations are presented in the following section). The results of the isotherm determination are presented in Table S5. The Average Relative Error (ARE) of each measurement was also calculated using eq. S17¹⁴ and is presented in Table S5.

$$ARE = \frac{100}{N} \sum_{i=1}^N \left| \frac{q_{meas} - q_{calc}}{q_{meas}} \right|_i \quad (S17)$$

In this equation, N is the number of data points, q_{meas} is the measured sorbed concentration at equilibrium, and q_{calc} is the calculated sorbed concentration based on the fitted parameters. The residual plots, presented in Figure S12 and Figure S13, show no discernible pattern, which means that the models are adequate.

Table S5: Results of the isotherm measurement

Adsorbent	Compound	Standard gas concentration, C (mol/m ³)	Slope of the curve, t _b vs. W (min/g)	R ²	W _e (g/g)	Sorbed concentration, q (mol/m ³)	Isotherm parameters (q = K C ^{1/n})			Isotherm parameters (C = a q ^b)	
							K	1/n	ARE (%)	a	b
Carbopack B	TCE	9.72 × 10 ⁻³	80.92	1.00	1.55 × 10 ⁻³	22.11	1355.06	0.62	3.44	9.48 × 10 ⁻⁶	1.60
		4.29 × 10 ⁻³	114.11	0.99	1.04 × 10 ⁻³	14.75					
		7.17 × 10 ⁻⁵	151.58	0.95	6.64 × 10 ⁻⁴	9.46					
		2.00 × 10 ⁻³	124.86	1.00	7.46 × 10 ⁻⁴	10.63					
		4.75 × 10 ⁻⁴	167.32	1.00	4.54 × 10 ⁻⁴	6.46					
Carbopack B	1,2,4-Trichloro benzene	4.56 × 10 ⁻⁴	3809.15	0.97	3.26 × 10 ⁻²	336.29	19995.09	0.56	7.81	1.87 × 10 ⁻⁸	1.80
		2.38 × 10 ⁻⁴	3870.50	0.99	1.73 × 10 ⁻²	178.03					
		6.38 × 10 ⁻⁴	2430.47	0.99	2.91 × 10 ⁻²	299.99					
		5.38 × 10 ⁻⁴	2765.70	1.00	2.79 × 10 ⁻²	288.12					
		4.24 × 10 ⁻⁴	3380.24	1.00	2.69 × 10 ⁻²	277.03					
Anasorb 747	Toluene	1.09 × 10 ⁻⁴	79675.00	1.00	8.24 × 10 ⁻²	1314.73	57204.45	0.41	3.47	2.52 × 10 ⁻¹²	2.44
		7.11 × 10 ⁻⁴	29112.00	0.99	1.97 × 10 ⁻¹	3137.71					
		1.70 × 10 ⁻³	16198.00	0.99	2.61 × 10 ⁻¹	4161.48					
		3.07 × 10 ⁻³	11053.00	0.99	3.22 × 10 ⁻¹	5138.16					
Anasorb 747	TCE	1.02 × 10 ⁻²	3220.92	0.99	4.45 × 10 ⁻¹	4982.89	18335.37	0.28	8.66	4.77 × 10 ⁻¹⁶	3.59
		1.41 × 10 ⁻³	15716.24	1.00	3.02 × 10 ⁻¹	3373.79					
		6.68 × 10 ⁻⁴	20407.18	1.00	1.85 × 10 ⁻¹	2072.26					
		3.23 × 10 ⁻⁴	41501.64	0.98	1.82 × 10 ⁻¹	2035.30					

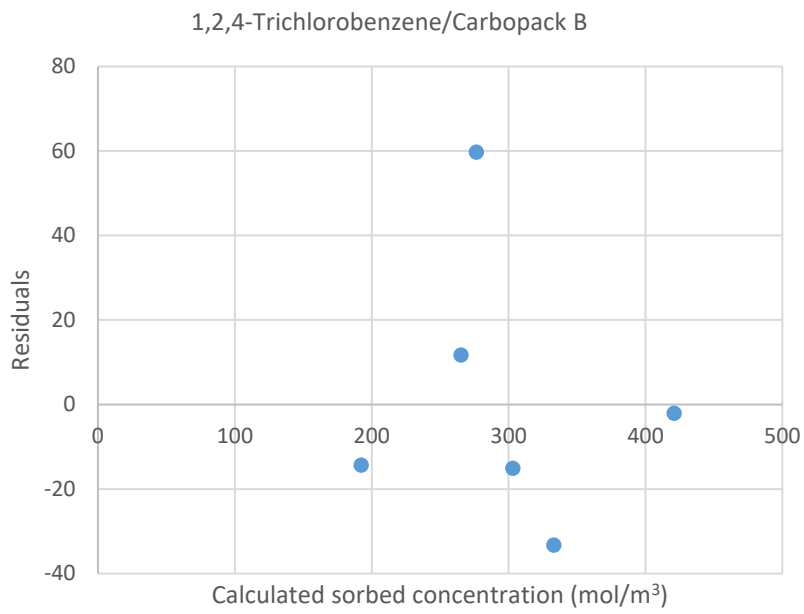
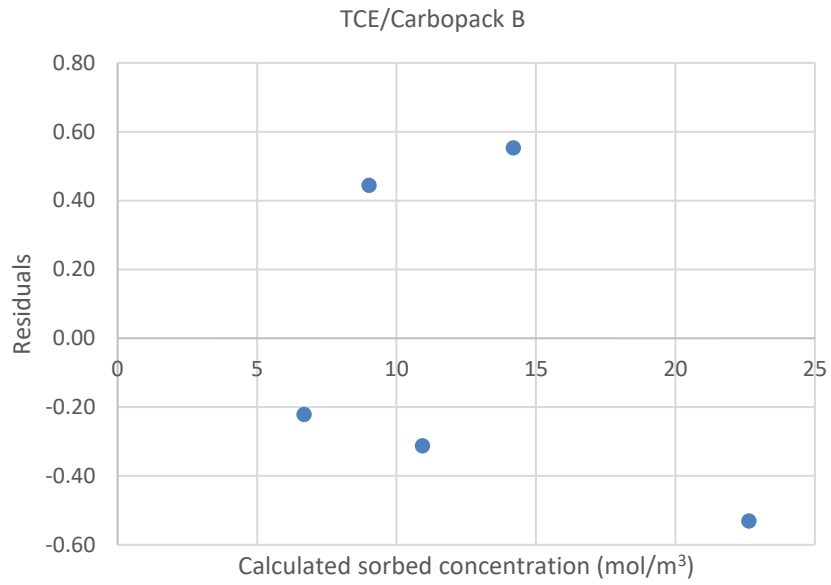


Figure S12: Plots of residuals for the fitted isotherm models for Carbopack B

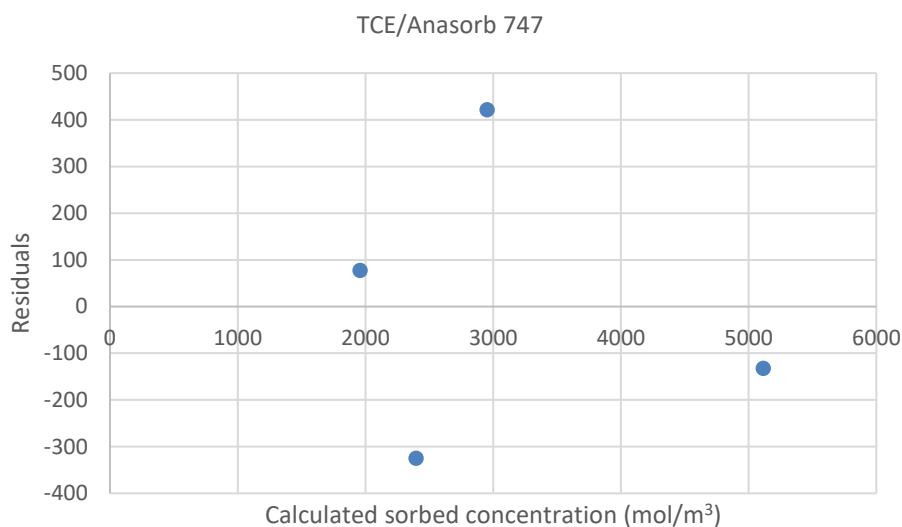
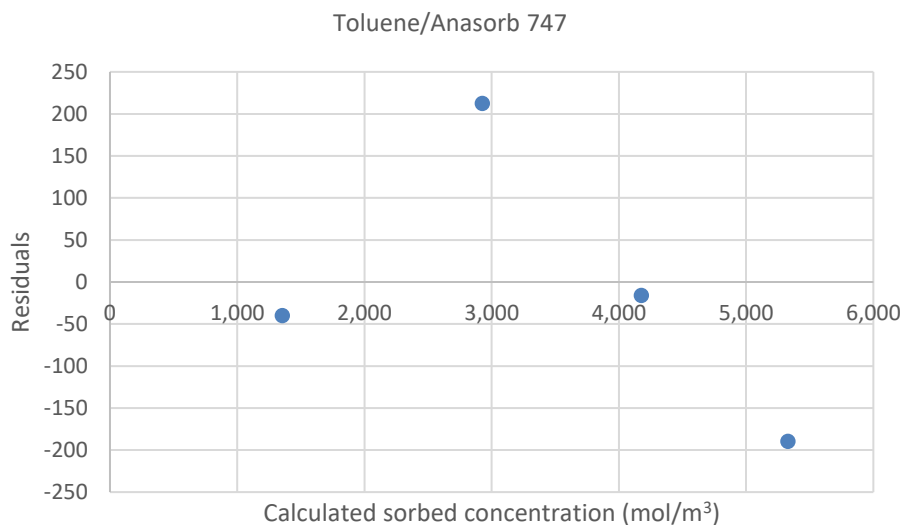


Figure S13: Plots of residuals for the fitted isotherm models for Anasorb 747

Characterization of Anasorb 747

Anasorb 747 was characterized using an Automated Gas Sorption Analyzer (Autosorb *iQ*) to determine the specific surface area, the pore size and the pore volume. The *BET* determination yielded a surface area of 1145.271 m²/g. The pore size distribution is presented in Figure S14. The results show major pore distribution below 2 nm of half pore width. An average value of the pore radius, using the Trapezoid rule, was calculated as follows:

$$\langle r \rangle = \frac{\int_{r_1}^{r_2} r dV_p dr}{\int_{r_1}^{r_2} dV_p dr} \quad (\text{S18})$$

r is the pore half width (pore radius assuming cylindrical pores), r_1 and r_2 are the smallest and largest values in the range of pore size distribution, and dV_p is the pore volume corresponding to the pore size per unit of mass ($\text{cm}^3/\text{\AA}/\text{g}$). This integration produced an average value of $\langle r \rangle = 0.5839$ nm for the half pore width.

The measured pore volume was $0.547 \text{ cm}^3/\text{g}$. To estimate the particle porosity and the solid density, calculations were done using the following steps: first, the average particle weight was measured to be 0.26 ± 0.06 mg (avg. \pm STD). The average particle volume was calculated to be 0.319 mm^3 ; therefore, the particle density, ρ_p , was found to be approximately 0.81 g/cm^3 by multiplying the pore volume value listed above by the particle density. The particle porosity, ε_μ , was found to be approximately 0.45, which is within the range of expected values. The solid density of the particles (ρ_s) was calculated using eq. S19, which yielded a value of 1.47 g/cm^3 .

$$\rho_s = \frac{\rho_p}{(1 - \varepsilon_\mu)} \quad (\text{S19})$$

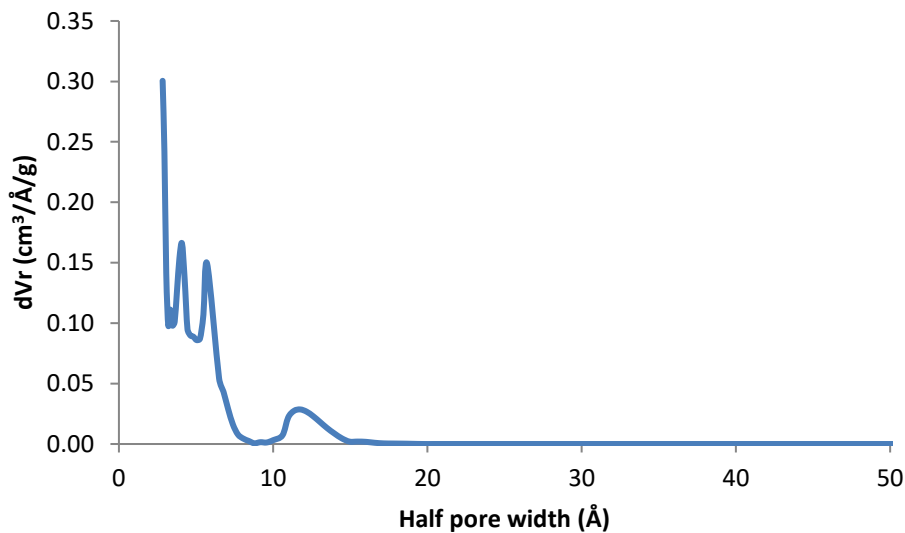


Figure S14: Pore size distribution for Anasorb 747

References

- 1 S. J. Lue, S. F. Wang, L. D. Wang, W. W. Chen, K. Du and S. Y. Wu, Diffusion of multicomponent vapors in a poly(dimethyl siloxane) membrane, *Desalination*, 2008, **233**, 277.
- 2 Y. Sun and J. Chen, Sorption/desorption properties of ethanol, toluene, and xylene in poly (dimethylsiloxane) membranes, *J Appl Polym Sci*, 1994, **51**, 1797.
- 3 K. S. Oh, Y. M. Koo and K. W. Jung, Characterization of a sheet membrane interface for sample introduction into a time-of-flight mass spectrometer, *Int. J. Mass Spectrom.*, 2006, **253**, 65.
- 4 E. Boscaini, M. L. Alexander, P. Prazeller and T. D. Mark, Investigation of fundamental physical properties of a polydimethylsiloxane (PDMS) membrane using a proton transfer reaction mass spectrometer (PTRMS), *Int. J. Mass Spectrom.*, 2004, **239**, 179.
- 5 K. Chao, V. Wang, H. Yang and C. Wang, Estimation of effective diffusion coefficients for benzene and toluene in PDMS for direct solid phase microextraction, *Polym. Test.*, 2011, **30**, 501.
- 6 A. Belles, C. Franke, C. Alary, Y. Aminot and J. W. Readman, Understanding and predicting the diffusivity of organic compounds in polydimethylsiloxane material for passive sampler applications using a simple quantitative structure–property relationship model, *Environ. Toxicol. Chem.*, 2018, **37**, 1291.
- 7 M. V. Chandak, Y. S. Lin, W. Ji and R. J. Higgins, Sorption and diffusion of volatile organic compounds in polydimethylsiloxane membranes, *J Appl Polym Sci*, 1998, **67**, 165.
- 8 A. Kloskowski, W. Chrzanowski, M. Pilarczyk and J. Namiesnik, Partition coefficients of selected environmentally important volatile organic compounds determined by gas-liquid chromatography with polydimethylsiloxane stationary phase, *J. Chem. Thermodyn.*, 2005, **37**, 21.
- 9 P. A. Martos, A. Saraullo and J. Pawliszyn, Estimation of air/coating distribution coefficients for solid phase microextraction using retention indexes from linear temperature-programmed capillary gas chromatography. application to the sampling and analysis of total petroleum hydrocarbons in air, *Anal. Chem.*, 1997, **69**, 402.
- 10 M. K. Shetty, M. A. Limmer, K. Waltermire, G. C. Morrison and J. G. Burken, In planta passive sampling devices for assessing subsurface chlorinated solvents, *Chemosphere*, 2014, **104**, 149.
- 11 ASTM International, *Standard Guide for Risk-Based Corrective Action Applied at Petroleum Release Sites*, E 1939-95 Reapproved 2015, West Conshohocken, PA, USA, 2015, www.astm.org/Standards/E1739.htm, (accessed July 2016).

12 G. A. Lugg, Diffusion coefficients of some organic and other vapors in air, *Anal. Chem.*, 1968, **40**, 1072.

13 N. Vahdat, P. M. Swearengen, J. S. Johnson, S. Priante, K. Mathews and A. Neidhardt, Adsorption capacity and thermal-desorption efficiency of selected adsorbents, *Am. Ind. Hyg. Assoc. J.*, 1995, **56**, 32.

14 K. Y. Foo and B. H. Hameed, Insights into the modeling of adsorption isotherm systems, *Chem. Eng. J.*, 2010, **156**, 2.